



Published in final edited form as:

*Genes Chromosomes Cancer*. 2011 October ; 50(10): 757–764. doi:10.1002/gcc.20897.

## Consistent t(1;10) with Rearrangements of *TGFBR3* and *MGEA5* in both Myxoinflammatory Fibroblastic Sarcoma and Hemosiderotic Fibrolipomatous Tumor

Cristina R Antonescu<sup>1</sup>, Lei Zhang<sup>1</sup>, G Petur Nielsen<sup>2</sup>, Andrew E Rosenberg<sup>2</sup>, Paola Dal Cin<sup>3</sup>, and Christopher DM Fletcher<sup>3</sup>

<sup>1</sup>Department of Pathology, Memorial Sloan-Kettering Cancer Center, New York, NY

<sup>2</sup>Department of Pathology, Massachusetts General Hospital, Boston, MA

<sup>3</sup>Department of Pathology, Brigham and Women's Hospital, Boston, MA

### Abstract

Despite their shared predilection for superficial soft tissue of distal extremities and frequent local recurrences, myxoinflammatory fibroblastic sarcoma (MIFS) and hemosiderotic fibrolipomatous tumor (HFLT) have distinct morphologic appearances. Recent studies have identified an identical t(1;10)(p22;q24) in 5 cases of MIFS and 2 of HFLT, as well as common amplifications on 3p11-12. In order to investigate further their potential relationship and to determine the incidence of t(1;10) in a larger cohort, we subjected 7 MIFS, 14 HFLT, and 3 cases with mixed morphology, to molecular and cytogenetic analysis. FISH analysis for rearrangements of *TGFBR3* on 1p22 and of *MGEA5* on 10q24 was performed in all cases, while the status of *VGLL3* gene amplification on 3p12.1 was investigated in 12 cases. Conventional karyotyping was performed in one HFLT and two cases with mixed MIFS/HFLT histology. Overall 83% of cases showed rearrangements in both *TGFBR3* and *MGEA5*. All three cases with mixed features of MIFS and HFLT were positive. Cytogenetic analysis performed in three cases confirmed an unbalanced der(10)t(1;10)(p22;q24). *VGLL3* gene amplification was noted in 10/12 cases of both histologies. The high incidence of t(1;10) in MIFS and HFLT reinforces a shared pathogenetic relationship. Furthermore, the co-existence of both components either synchronously or metachronously in a primary or subsequent recurrence, suggest either different morphologic variants or different levels of tumor progression of a single biologic entity. FISH analysis for *TGFBR3* and *MGEA5* rearrangements can be applied as a reliable diagnostic molecular test when confronted with limited material or a challenging diagnosis.

### Keywords

sarcoma; translocation; soft tissue; myxoinflammatory; hemosiderotic

### INTRODUCTION

Myxoinflammatory fibroblastic sarcoma (MIFS) is a rare low-grade sarcoma with predilection for the subcutaneous tissues of distal extremities, associated clinically with repeated local recurrences, but rare metastases (Meis-Kindblom and Kindblom, 1998; Michal, 1998; Montgomery et al., 1998). Morphologically, MIFS has distinctive features, including a multinodular architecture with alternating myxoid and cellular areas, a

prominent inflammatory infiltrate, a variable number of mono and multinucleate Reed-Sternberg-like tumor cells that have prominent viral inclusion-like nucleoli and mucin-containing pseudolipoblasts.

In contrast, hemosiderotic fibrolipomatous tumor (HFLT) arises with predilection in the subcutaneous tissue of the ankle in middle-aged women. It is a predominantly fatty lesion with a complex admixture of bland fibroblastic spindle cells, multinucleated giant cells and often abundant hemosiderin deposits and lymphoid aggregates. HFLT was initially thought to represent a reactive process, because of the presence of the inflammatory and polymorphous fibrohistiocytic infiltrate, as well as a history of prior trauma (Marshall-Taylor and Fanburg-Smith, 2000). Subsequently, several series documented that HFLT has a high propensity for local recurrence, and antecedent trauma is not as common as previously believed, therefore it was reclassified as a neoplastic process (Browne and Fletcher, 2006).

Despite these morphologic differences between MIFS and HFLT these neoplasms have been shown to have similar genetic alterations. A recurrent t(1;10)(p22;q24) has been identified in 5 cases of MIFS and 2 cases of HFLT (Lambert et al., 2001; Wettach et al., 2008; Hallor et al., 2009). Interestingly, the same t(1;10)(p22;q24) was found in a soft tissue tumor that demonstrated hybrid features of MIFS/HFLT (Elco et al., 2010). The breakpoints of this translocation have been mapped to *TGFBR3* in 1p22 and in *MGEA5* in 10q24 (Hallor et al., 2009). Despite that both of these tumors have the same translocation, non-random chromosome 3 abnormalities or amplifications of chromosome 3p11-12 material, in the form of ring and markers chromosomes, have been reported as a common event in MIFS (Mansoor et al., 2004; Baumhoer et al., 2007; Hallor et al., 2009), but not in HFLT (Wettach et al., 2008).

To further determine the pathogenetic relationship between MIFS and HFLT we used FISH analysis to investigate rearrangements of these genes in a larger cohort of MIFS, HFLT and tumors with mixed morphology. In addition, we assessed the incidence of *VGLL3* amplification on 3p.12.1 in the same cohort.

HFLT also exhibits some morphologic overlap with the so-called 'early phase' of pleomorphic hyalinizing angiectatic tumor (PHAT), therefore, some authors have suggested that they may represent a morphologic continuum (Folpe and Weiss, 2004). Accordingly, we also tested 3 PHAT cases for *TGFBR3* and *MGEA5* gene rearrangements, as well as for *VGLL3* amplifications by FISH.

## MATERIAL AND METHOD

### Patients and Tumor Characteristics

The 7 patients with MIFS had no gender predilection (4 females, 3 males), and their ages ranged from 29–58 years (median 36, mean 42). The tumors were equally distributed between the upper (hand/fingers, 3) and lower extremities (foot/ankle, 4)(Fig. 1A). Microscopically, the tumors had a nodular growth pattern and were composed of spindle cells with variable degree of nuclear pleomorphism, embedded in a pronounced myxoid stroma (Fig. 1B). Pseudolipoblasts, Reed-Sternberg-like cells or cells with large inclusion-type nucleoli were consistently present admixed within a rich inflammatory infiltrate (Fig. 1C).

The 14 patients with HFLT had a strong female predilection (12 females, 2 males), and their ages ranged from 32–62 years (median 43, mean 45). The tumors typically arose in the lower extremity, with only one patient having an upper extremity (hand/finger) lesion. All tumors were located in the subcutaneous tissue and had infiltrative margins. Microscopically, the

tumors were composed of fascicles of bland fibroblastic cells, admixed in a complex fashion with mature adipose tissue. (Fig. 1D). Other consistent features included multinucleated giant cells, a high content of hemosiderin pigment (Fig. 1E) and lymphocytic infiltrate. However, the tumors showed variability in respect to the proportion of each of these components. As such, predominantly fatty lesions showed only a focal fibrohistiocytic infiltrate that was distributed in a honeycomb pattern reminiscent of either an atypical lipomatous tumor or a dermatofibrosarcoma protuberans. Conversely, tumors showing more nodular or confluent solid fibrohistiocytic areas, with multinucleated giant cells and abundant hemosiderin pigment, resembled other fibrohistiocytic lesion, such as diffuse tenosynovial giant cell tumor. Quite frequently the HFLT contained a rich vascular network composed of medium sized blood vessels that were most numerous in the fat at the periphery of the lesions (Fig. 1F). However, the tumors lacked the thick hyalinized walls and fibrinoid changes often seen within the vascular component of classic PHAT. Furthermore, the lesional cells lacked the degree of nuclear pleomorphism commonly seen in PHAT.

In two patients, the primary tumors showed a mixture of MIFS and HFLT components. Thus, myxoid nodules with atypical cells with virocyte-type inclusions showed a gradual transition to an infiltrative HFLT component (Figs. 1G,H). In a third patient, a 60 year old female, the primary foot lesion was composed only of HFLT, while the subsequent recurrent lesion, 9 years later, showed only a MIFS appearance.

The 3 patients with PHAT included one female and two males, with an age range of 45–79 years (mean 57). The tumor location included two in the thigh and one in the leg. Histologically, they exhibited the typical appearance of a spindle and focally pleomorphic cellular proliferation associated with a conspicuous and distinctive vascular tree that demonstrated marked hyalinization and fibrinoid changes within their walls (Fig. 1I). The degree of nuclear pleomorphism varied from focal to severe, and many of the large atypical cells contained intra-nuclear inclusions. In one of the three cases (45 year old female with a thigh mass), the central portion of the tumor had the appearance of classic PHAT, whereas, the periphery of the lesion was composed of a less-cellular component, infiltrating the adjacent fat (Fig. 1J). This latter pattern simulated the appearance of HFLT and was consistent with what was previously described as ‘early PHAT’ (Fig 1K).

The control group consisted of three cases of other sarcoma types involving the soft tissues of the hands and feet, including two cases of high grade malignant fibrous histiocytoma/undifferentiated pleomorphic sarcoma with an inflammatory component and one high grade sarcoma with myofibroblastic differentiation.

### **Cytogenetic Analysis and Fluorescence In Situ Hybridization (FISH)**

GTG banded karyotyping was performed in 3 cases, using standard procedures. BAC clones were chosen according to the UCSC genome browser (<http://genome.ucsc.edu>).

The BAC clones were obtained from BACPAC sources of Children’s Hospital of Oakland Research Institute (CHORI) (Oakland, CA) (<http://bacpac.chori.org>) (Table S1, Fig. 2). FISH was performed as previously described (Antonescu et al., 2010). In brief, DNA from individual BACs was isolated according to the manufacturer’s instructions, labeled with different fluorochromes in a nick translation reaction and the probes were validated on normal human metaphases. Probe mixtures were denatured, and hybridized to pretreated slides. Slides were incubated, washed and mounted with DAPI in an antifade solution. At least two hundred successive non-overlapping nuclei were examined using a fluorescence microscope. A case was confirmed as positive for rearrangement of a given gene when 20% of the nuclei examined showed a break-apart signal pattern using its respective BAC probes. Gene amplification was defined by the presence of tight signal clusters and a gene/

reference probe per cell ratio two, or 10 copies of the gene per cell in 10% of analyzed cells.

## RESULTS

### Cytogenetic analysis

GTG banded karyotypes were obtained in one HFLT and two cases with mixed morphology. The HFLT showed a rather simple karyotype, with an apparently balanced  $t(1;10)(p22;q24)$  and a deletion of 3p11 (Fig. 3A of the partial karyotype). Although only six abnormal metaphases were obtained from one of the tumors with mixed MIFS and HFLT morphology, the two abnormal clones (Fig. 4A,B) as well as the two single abnormal metaphases (Fig. 4C,D) showed a similar  $der(10)$  evolving from a  $t(1;10)$ , with different abnormalities in chromosomes 1 and 3.

The karyotype from the second tumor with mixed morphology showed several aberrations, including an unbalanced translocation involving chromosomes 1 and 3,  $der(1)t(1;3)(p11;q11)$ , a balanced  $t(6;15)(p21;q26)$ , an unbalanced translocation involving chromosomes 1 and 10,  $der(10)t(1;10)(p22;q24)$ , and a few copies of an apparently similar ring chromosome of unknown origin, as previously published (Elco et al., 2010).

### Consistent unbalanced *TGFBR3* and *MGEA5* rearrangements in MIFS and HFLT

In the MIFS group, 5 of the 7 cases tested by FISH showed the presence of rearrangements in both *TGFBR3* and *MGEA5* (Fig. 2A,B). In all cases, however, the rearrangement pattern observed was unbalanced, with loss of the centromeric part of *TGFBR3* and deletion of the telomeric part of *MGEA5* (Figs. 2A, B). Two cases were negative for both gene rearrangements, one case in the foot and one in the hand. Both negative cases showed a typical morphologic appearance on careful re-review.

In the HFLT group, 12 of the 14 cases were positive for *TGFBR3* and *MGEA5* gene rearrangements with a similar unbalanced pattern, as described above and illustrated in Figs. 3B,C. The lack of *TGFBR3* and/or *MGEA5* rearrangements by FISH in two cases from each group could be related to the high number of reactive inflammatory cells relative to the low content of lesional cells.

In all three cases with mixed morphology, the FISH studies showed similar *TGFBR3* rearrangements with deletion of the centromeric part and *MGEA5* rearrangement with deletion of the telomeric part (Fig. 3D).

No gene abnormalities in either *TGFBR3* or *MGEA5* were detected by FISH in the 3 PHAT lesions or the 3 cases of other sarcoma types tested.

### Amplification of *VGLL3* is a common event in both MIFS and HFLT, but not in PHAT

In 12 cases adequate material was available to investigate the copy number alterations at the *VGLL3* locus on 3p.12.1 by FISH (Hallor et al., 2009). High level amplification (Fig. 2C) was present in 10 of the 12 cases tested, including 2/4 MIFS, 5/5 HFLT and 3/3 cases with mixed morphology. None of the three cases of PHAT showed copy number alterations of *VGLL3*.

## DISCUSSION

Despite their common presentation in superficial soft tissues of the distal extremities and frequent local recurrences, MIFS and HFLT have distinct morphologies. However, the recent identification of the same  $t(1;10)$  genetic abnormality raised the question of a

pathogenetic link between MIFS, a low grade sarcoma, and HFLT, a lesion in which the neoplastic nature was at least initially under question (Hallor et al., 2009).

HFLT occurs mainly in the ankle region of older females (Marshall-Taylor and Fanburg-Smith, 2000). The fatty component typically predominates and is composed of homogeneously sized adipocytes resembling normal fat. The spindle cell proliferation shows a polymorphous phenotype and varies from thin septa with a honey-comb growth pattern within fat to more confluent solid areas. None of our cases showed large pleomorphic cells with pseudonuclear inclusions or blood vessels with fibrinoid changes in their walls to suggest a morphologic overlap with the classic PHAT appearance. However, the so-called 'early PHAT' component, occurring at the periphery of classic PHAT lesions, share significant overlap to the HFLT. As such, previous reports speculated that HFLT is the same process as the early phase of PHAT and may represent the precursor lesion of classic PHAT (Folpe and Weiss, 2004). Furthermore, both lesions have a similar immunophenotype, in that the neoplastic cells express CD34. Other investigators have suggested that the PHAT-like morphology might be shared by a number of other neoplasms and may not represent a distinctive entity (Elco et al., 2010; Moretti et al., 2010). Our findings, demonstrating the absence of *TGFBR3* or *MGEA5* gene rearrangements in the three PHAT tumors tested (including one example containing the previously described 'early' PHAT pattern), suggest a different pathogenesis and do not provide support for a morphologic continuum between the precursor PHAT lesion and HFLT.

Although most translocations in sarcomas result in functional gene fusions, our data support previous results suggesting that both *TGFBR3* and *MGEA5* candidates for the gene fusion are transcribed in opposite directions and thus unable to form a fusion transcript (Hallor et al., 2009). Based on the unbalanced pattern noted from both FISH and cytogenetics testing, at mRNA level both *TGFBR3* and *MGEA5* lost their 5' sequences, while the der(10) chromosome contains the residual 3' sequences from *TGFBR3* and *MGEA5*. Furthermore, the expression levels of both *TGFBR3* and *MGEA5* do not appear altered by either gene expression analysis or real time quantitative PCR (Hallor et al., 2009). As overexpression of FGF8 on 10q was identified by microarray analysis, investigators have suggested that the t(1;10) may alter gene transcription away from the breakpoint. FGF8 expression during embryogenesis is tightly regulated and it is transcriptionally silent in adult tissues (Thisse and Thisse, 2005; Valta et al., 2006). Reactivation of FGF8 has been found in a variety of epithelial malignancies as well as in synovial sarcoma (Tanaka et al., 1998; Ishibe et al., 2005). Similar ectopic expression of proto-oncogenes secondary to position effects has been reported in other translocation-associated malignancies, such as myeloid leukemia with either t(4;12) or t(5;12) with up regulation of *ETV6* (Cools et al., 2002).

In addition to t(1;10), a subset of MIFS have been reported to show ring or marker chromosomes secondary to 3p11.1-12.1 amplifications (Mansoor et al., 2004; Hallor et al., 2009). Ring and marker chromosomes have been described in other low grade sarcomas, either due to amplified 12q13-15 material (well-differentiated liposarcoma, parosteal osteosarcoma) or secondary to tandem repeats of the t(17;22) breakpoint region in dermatofibrosarcoma protuberans (Naeem et al., 1995). More recently, amplification of 3p11.1-12.1 chromosome material by BAC array CGH was detected in 19 samples of 404 soft tissue sarcomas (Helias-Rodzewicz et al., 2010). Most of these tumors were high grade and were either retroperitoneal dedifferentiated liposarcomas or undifferentiated pleomorphic sarcomas of the extremities (Helias-Rodzewicz et al., 2010). By array CGH studies, the amplicon harbored three genes, *VGLL3*, *CHMP2B* and *POU1F1* (Hallor et al., 2009; Helias-Rodzewicz et al., 2010). Additionally, *VGLL3* and *CHMP2B* showed overexpression by gene expression profiling and real-time PCR (Hallor et al., 2009). By Genome-Wide Human SNP Array 6.0 on a different series of sarcomas, 6 of 132 tumors had

amplification of 3p, with only *VGLL3* in common (Helias-Rodzewicz et al., 2010). Further validation by quantitative genomic PCR and Affymetrix expression data showed good correlation between *VGLL3* gene amplification and expression levels (Helias-Rodzewicz et al., 2010). Our findings confirm the presence of high level *VGLL3* amplification by FISH in MIFS, as well as in HFLT and cases with mixed morphology, suggesting a potential pathogenetic role in this tumor type. *VGLL3* encodes proteins that are the cofactors of the TEAD family of transcription factors (Vaudin et al., 1999).

In summary, the high incidence of t(1;10)(p22; q24) identified in both MIFS and HFLT in our study reinforces their shared pathogenetic relationship. Furthermore, the coexistence of both components either synchronously or metachronously in primary lesions or a subsequent recurrence, suggest either different morphologic variants or different levels of tumor progression of a single entity. FISH analysis for *TGFBR3* and *MGEA5* rearrangements can be applied as a reliable molecular test when confronted with limited biopsy material or a challenging diagnosis. Frequent high level amplification of *VGLL3* on 3p12 was also identified in most cases of both morphologic types, in further support of their shared pathogenesis.

## Supplementary Material

Refer to Web version on PubMed Central for supplementary material.

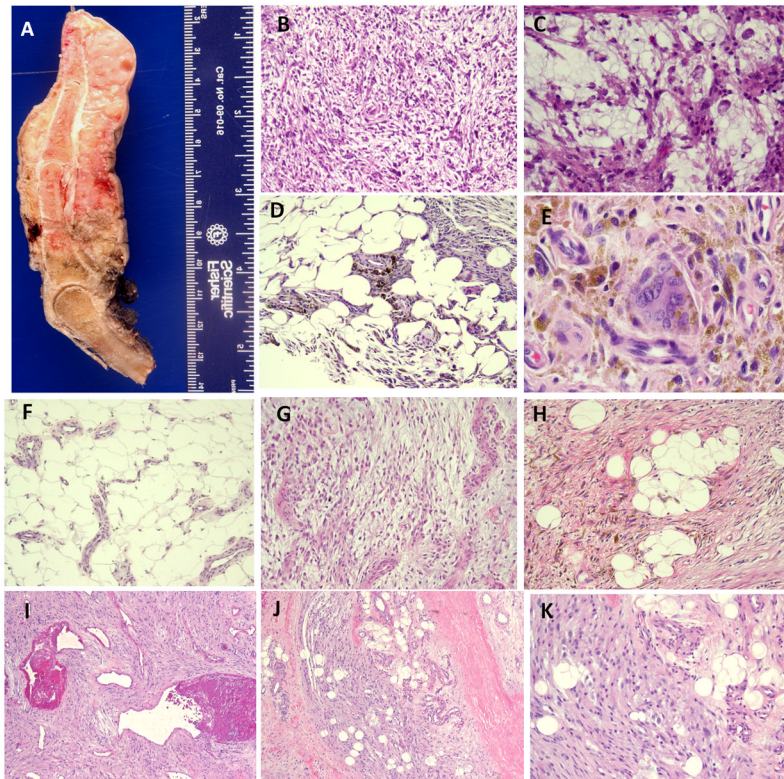
## Acknowledgments

Supported by: PO1 CA047179-15A2 (CRA) and P50 CA 140146-01 (CRA)

## References

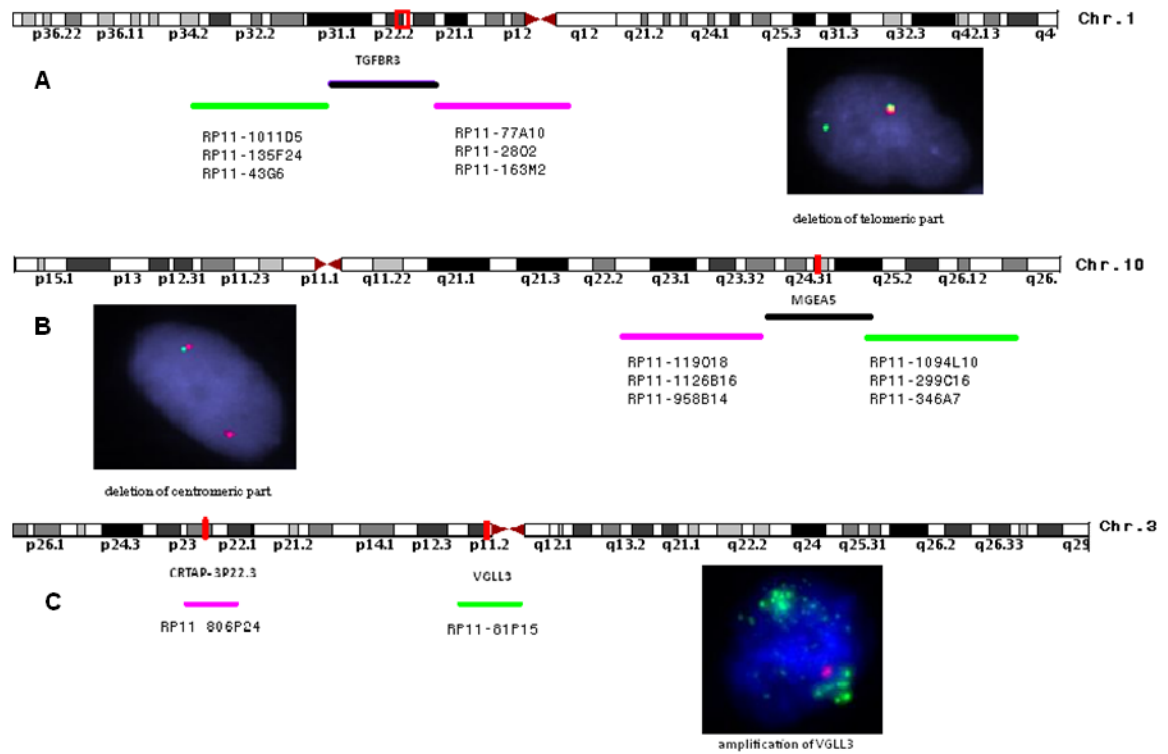
- Antonescu CR, Zhang L, Chang NE, Pawel BR, Travis W, Katabi N, Edelman M, Rosenberg AE, Nielsen GP, Dal Cin P, Fletcher CD. EWSR1-POU5F1 fusion in soft tissue myoepithelial tumors. A molecular analysis of sixty-six cases, including soft tissue, bone, and visceral lesions, showing common involvement of the EWSR1 gene. *Genes Chromosomes Cancer*. 2010; 49:1114–1124. [PubMed: 20815032]
- Baumhoer D, Glatz K, Schulten HJ, Fuzesi L, Fricker R, Kettelhack C, Hasenboehler P, Oberholzer M, Jundt G. Myxoinflammatory fibroblastic sarcoma: investigations by comparative genomic hybridization of two cases and review of the literature. *Virchows Arch*. 2007; 451:923–928. [PubMed: 17694321]
- Browne TJ, Fletcher CD. Haemosiderotic fibrolipomatous tumour (so-called haemosiderotic fibrohistiocytic lipomatous tumour): analysis of 13 new cases in support of a distinct entity. *Histopathology*. 2006; 48:453–461. [PubMed: 16487368]
- Cools J, Mentens N, Odero MD, Peeters P, Wlodarska I, Delforge M, Hagemeijer A, Marynen P. Evidence for position effects as a variant ETV6-mediated leukemogenic mechanism in myeloid leukemias with a t(4;12)(q11–q12;p13) or t(5;12)(q31;p13). *Blood*. 2002; 99:1776–1784. [PubMed: 11861295]
- Elco CP, Marino-Enriquez A, Abraham JA, Dal Cin P, Hornick JL. Hybrid myxoinflammatory fibroblastic sarcoma/hemosiderotic fibrolipomatous tumor: report of a case providing further evidence for a pathogenetic link. *Am J Surg Pathol*. 2010; 34:1723–1727. [PubMed: 20871391]
- Folpe AL, Weiss SW. Pleomorphic hyalinizing angiectatic tumor: analysis of 41 cases supporting evolution from a distinctive precursor lesion. *Am J Surg Pathol*. 2004; 28:1417–1425. [PubMed: 15489645]
- Hallor KH, Sciot R, Staaf J, Heidenblad M, Rydholm A, Bauer HC, Astrom K, Domanski HA, Meis JM, Kindblom LG, Panagopoulos I, Mandahl N, Mertens F. Two genetic pathways, t(1;10) and amplification of 3p11–12, in myxoinflammatory fibroblastic sarcoma, haemosiderotic

- fibrolipomatous tumour, and morphologically similar lesions. *J Pathol.* 2009; 217:716–727. [PubMed: 19199331]
- Helias-Rodzewicz Z, Perot G, Chibon F, Ferreira C, Lagarde P, Terrier P, Coindre JM, Aurias A. YAP1 and VGLL3, encoding two cofactors of TEAD transcription factors, are amplified and overexpressed in a subset of soft tissue sarcomas. *Genes Chromosomes Cancer.* 2010; 49:1161–1171. [PubMed: 20842732]
- Ishibe T, Nakayama T, Okamoto T, Aoyama T, Nishijo K, Shibata KR, Shima Y, Nagayama S, Katagiri T, Nakamura Y, Nakamura T, Toguchida J. Disruption of fibroblast growth factor signal pathway inhibits the growth of synovial sarcomas: potential application of signal inhibitors to molecular target therapy. *Clin Cancer Res.* 2005; 11:2702–2712. [PubMed: 15814652]
- Lambert I, Debiec-Rychter M, Guelinckx P, Hagemeyer A, Sciort R. Acral myxoinflammatory fibroblastic sarcoma with unique clonal chromosomal changes. *Virchows Arch.* 2001; 438:509–512. [PubMed: 11407481]
- Mansoor A, Fidda N, Himoe E, Payne M, Lawce H, Magenis RE. Myxoinflammatory fibroblastic sarcoma with complex supernumerary ring chromosomes composed of chromosome 3 segments. *Cancer Genet Cytogenet.* 2004; 152:61–65. [PubMed: 15193443]
- Marshall-Taylor C, Fanburg-Smith JC. Hemosiderotic fibrohistiocytic lipomatous lesion: ten cases of a previously undescribed fatty lesion of the foot/ankle. *Mod Pathol.* 2000; 13:1192–1199. [PubMed: 11106076]
- Meis-Kindblom JM, Kindblom LG. Acral myxoinflammatory fibroblastic sarcoma: a low-grade tumor of the hands and feet. *Am J Surg Pathol.* 1998; 22:911–924. [PubMed: 9706971]
- Michal M. Inflammatory myxoid tumor of the soft parts with bizarre giant cells. *Pathol Res Pract.* 1998; 194:529–533. [PubMed: 9779486]
- Montgomery EA, Devaney KO, Giordano TJ, Weiss SW. Inflammatory myxohyaline tumor of distal extremities with virocyte or Reed-Sternberg-like cells: a distinctive lesion with features simulating inflammatory conditions, Hodgkin's disease, and various sarcomas. *Mod Pathol.* 1998; 11:384–391. [PubMed: 9578090]
- Moretti VM, de la Cruz M, Brooks JS, Lackman RD. Early pleomorphic hyalinizing angiectatic tumor: precursor or distinct lesion? *Orthopedics.* 2010; 33:516. [PubMed: 20608621]
- Naeem R, Lux ML, Huang SF, Naber SP, Corson JM, Fletcher JA. Ring chromosomes in dermatofibrosarcoma protuberans are composed of interspersed sequences from chromosomes 17 and 22. *Am J Pathol.* 1995; 147:1553–1558. [PubMed: 7495279]
- Tanaka A, Furuya A, Yamasaki M, Hanai N, Kuriki K, Kamiakito T, Kobayashi Y, Yoshida H, Koike M, Fukayama M. High frequency of fibroblast growth factor (FGF) 8 expression in clinical prostate cancers and breast tissues, immunohistochemically demonstrated by a newly established neutralizing monoclonal antibody against FGF 8. *Cancer Res.* 1998; 58:2053–2056. [PubMed: 9605740]
- Thisse B, Thisse C. Functions and regulations of fibroblast growth factor signaling during embryonic development. *Dev Biol.* 2005; 287:390–402. [PubMed: 16216232]
- Valta MP, Hentunen T, Qu Q, Valve EM, Harjula A, Seppanen JA, Vaananen HK, Harkonen PL. Regulation of osteoblast differentiation: a novel function for fibroblast growth factor 8. *Endocrinology.* 2006; 147:2171–2182. [PubMed: 16439448]
- Vaudin P, Delanoue R, Davidson I, Silber J, Zider A. TONDU (TDU), a novel human protein related to the product of vestigial (vg) gene of *Drosophila melanogaster* interacts with vertebrate TEF factors and substitutes for Vg function in wing formation. *Development.* 1999; 126:4807–4816. [PubMed: 10518497]
- Wettach GR, Boyd LJ, Lawce HJ, Magenis RE, Mansoor A. Cytogenetic analysis of a hemosiderotic fibrolipomatous tumor. *Cancer Genet Cytogenet.* 2008; 182:140–143. [PubMed: 18406878]

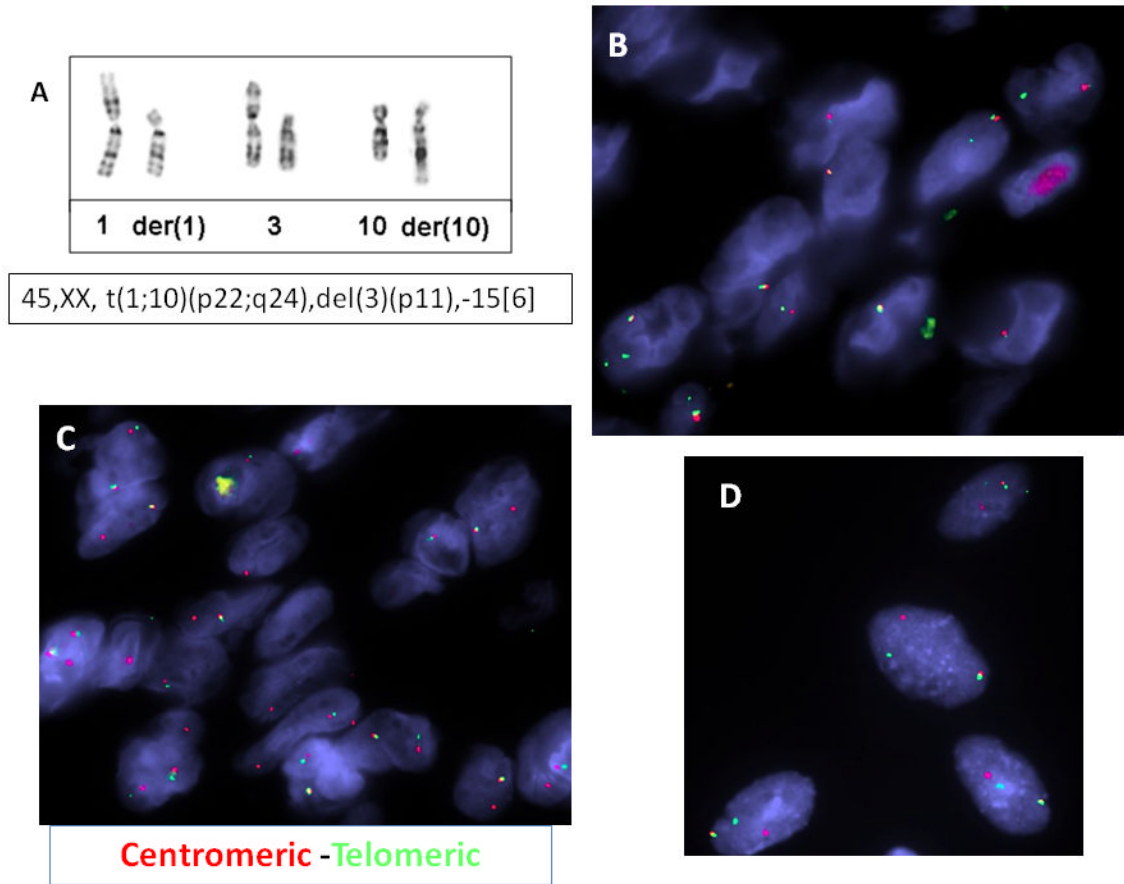


**Figure 1.** Pathologic appearance of the investigational and control groups. A. Ray amputation specimen showing a 7 cm circumferential subcutaneous MIFS, with a fleshy tan cut surface; which showed microscopically a spindle and pleomorphic cellular proliferation embedded in a myxoid stroma (B, 200 $\times$ ), with pseudo-lipoblasts and inclusion type nucleoli (C, 400 $\times$ ); HFLT composed of mature adipose fat infiltrated by a bland spindle cell proliferation (D, 100 $\times$ ), showing abundant hemosiderin-deposition and multinucleated giant cells (E, 400 $\times$ ); increased vascular proliferation composed of medium sized blood vessels is a common finding at the periphery of HFLT (F, 100 $\times$ ); 44 ear old female with a foot lesion showing areas of MIFS (G, 100 $\times$ ), blending with areas of HFLT (H, 100 $\times$ ). From the control group, one PHAT tumor from the thigh of a 45 year old female, showed the classic appearance of spindle cells with distinct pleomorphism and fibrinoid changes within dilated blood vessels (I, 100 $\times$ ); in addition, at the periphery of the lesion, an infiltrative component within the fat known as ‘early PHAT’, resembled the HFLT appearance (J, 200 $\times$ ; K, 400 $\times$ , inset).



**Figure 2.**

Distribution of BAC probe sets tested, flanking: A. *TGFBR3* on 1p22, inset shows a pair of fused normal signals, and a single green signal, suggesting deletion of the centromeric red signal; B. *MGEA5* on 10q24, inset showing loss of the green, telomeric part and by FISH; and C. *VGLL3* (probe covering the gene in green) on 3p12.1, inset showing high level amplification in a MIFS lesion (probe at 3p22.1 in red used as reference).

**Figure 3.**

Cytogenetic and FISH results in HFLT. A. Partial karyotype showing an apparently balanced t(1;10)(p22;q24) in a HFLT foot lesion from a 32 year-old female; which by FISH showed the presence of *TGFBR3* gene rearrangement, with the deletion of the centromeric part (B, red) and *MGEA5* rearrangement with the deletion of the telomeric part (C, green). FISH analysis using centromeric *MGEA5* (red) and telomeric *TGFBR3* (green) probes showed a fused signal in a 42 year-old female with a left ankle lesion with mixed MIFS/HFLT morphology (D).

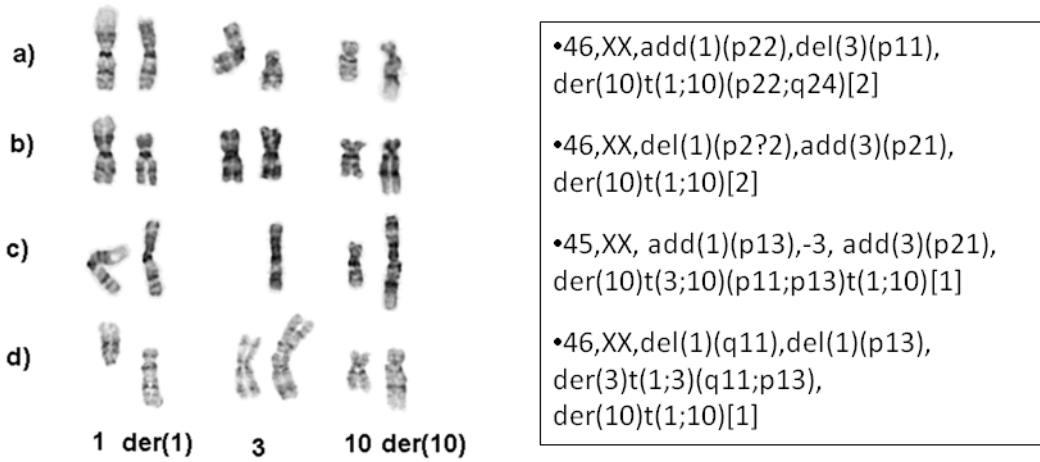


**Figure 4.** Partial GTG banded karyotype of a tumor with mixed MIFS/HFLT morphologic appearance. The two clonal populations (A,B) as well as the single abnormal metaphases (C,D) showed consistent der(10) evolving from a t(1;10), but variable alterations in chromosomes 1 and 3.